CSIRO PUBLISHING

Australian Journal of Physics

Volume 52, 1999

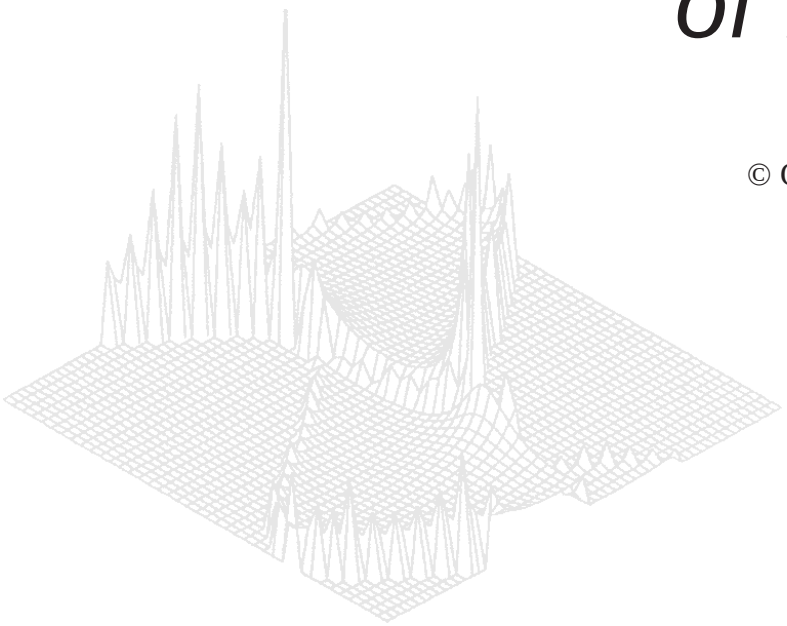

A journal for the publication of
original research in all branches of physics

www.publish.csiro.au/journals/ajp

All enquiries and manuscripts should be directed to
Australian Journal of Physics
CSIRO PUBLISHING
PO Box 1139 (150 Oxford St)
Collingwood Telephone: 61 3 9662 7626
Vic. 3066 Facsimile: 61 3 9662 7611
Australia Email: peter.robertson@publish.csiro.au

Published by **CSIRO** PUBLISHING
for CSIRO Australia and
the Australian Academy of Science

Aust. J. Phys., 1999, **52**, 363–76

Understanding Multicentre Electron Orbitals by Electron Momentum Spectroscopy*

Ian E. McCarthy[A] *and Maarten Vos*[B]

[A]Department of Physics, Flinders University of South Australia,
GPO Box 2100, Adelaide, SA 5001, Australia.
[B]Research School of Physical Sciences and Engineering,
Australian National University, Canberra, ACT 0200, Australia.

Abstract

Electron momentum spectroscopy can investigate qualitative predictions based on a physical understanding of the one-electron structure of a system. We describe examples of this understanding for molecules and solids.

1. Introduction

Since 1973 electron momentum spectroscopy (EMS) has proved to be a probe of unprecedented power and scope for investigating the validity of different types of self-consistent-field (SCF) calculations of electron orbitals in atoms and molecules (McCarthy and Weigold 1991). At external-electron energies so high that the derived structure information is independent of energy, the distribution of recoil momentum is equal to the absolute square of the momentum-space overlap of the energy-selected final electronic state with the electronic ground state of the target. This is a one-electron function called the quasiparticle or Dyson orbital in momentum space:

$$\phi_\alpha(\mathbf{q}) = (2\pi)^{-3/2} \int d^3r \exp(-i\mathbf{q}\cdot\mathbf{r})\psi_\alpha(\mathbf{r}). \quad (1)$$

Its absolute square, which is spherically averaged for randomly-oriented targets, gives the density for the momentum $\mathbf{q}$, corresponding to the orbital energy $\epsilon(\mathbf{q})$. The orbital in coordinate space is $\psi_\alpha(\mathbf{r})$, where the subscript α denotes the symmetry.

EMS has recently been applied to crystalline and amorphous solids (Vos and McCarthy 1995). In the application to crystals the quantity of physical interest is the orbital of the unit cell, described for example by equation (8·6) of Ashcroft and Mermin (1976). Its relationship to the orbitals of the crystal is described in Section 4. Here the orbital energy is related to the momentum by the dispersion relation for the electron band (Ashcroft and Mermin 1976) denoted by α. The experiment observes the energy–momentum density for the band.

* Refereed paper based on a contribution to the Australia–Germany Workshop on Electron Correlations held in Fremantle, Western Australia, on 1–6 October 1998.

 10.1071/PH98078 0004-9506/99/030363$05.00

For an atomic or molecular target the experimental definition of an occupied orbital arises from the identification of orbital manifolds of ion states, all of which have momentum density profiles of the same shape and of magnitude proportional to the spectroscopic factor for the state. Spectroscopic factors for each completely-observed manifold sum to the same number, which is normalised to 1. This is the spectroscopic sum rule. The momentum-density shape characterises the Dyson orbital, which is normalised by the sum rule.

The experimental definition of the occupied orbitals is of course unique, unlike various theoretical definitions that are used for convenient basis sets. It may be complemented by a unique definition of unoccupied orbitals derived from the potential that gives the occupied ones. Correlated many-body wave functions are defined as linear combinations of configurations constructed in the form of determinants of orbitals. Excited configurations have holes in the fully-occupied configuration that release particles to the unoccupied orbitals. The unique definition of orbitals is therefore the necessary starting point for the unique definition of correlations. The spectroscopic factors provide a strong constraint on the correlations.

The investigation of the validity of *ab initio* orbital calculations requires little physical understanding of the structure of the orbitals. One needs only to know how to write a large Schrödinger equation and to have some idea of the mathematical and numerical techniques that have gone into writing the computer program for the orbitals. However, EMS can also investigate qualitative predictions based on a physical understanding of the structure of a system. We describe some examples of this understanding for molecules and solids.

2. The Hydrogen Molecule

The simplest multinucleus system is the hydrogen molecule. It is a prototype for understanding the chemical bond. In molecules and solids chemical bonds are understood in terms of linear combinations of atomic orbitals. The orbitals are convenient mathematical functions, not exactly those of free atoms, but this does not influence our considerations.

In order to understand the hydrogen-molecule bond (Ruedenberg 1962), we compare the space distribution of charge with that of two hydrogen atoms at the internuclear distance of the molecule, $1{\cdot}4$ a.u. The symmetric combination of two 1s orbitals has lower potential energy in the overlap region between the two nuclei, since it puts increased negative charge there. It also has lower kinetic energy in this region, since the volume occupied by the electron charge is larger and the density gradients, which determine the absolute momentum, are smaller. The redistribution of charge results in reduced density near each nucleus. The reduced charge cloud is attracted more strongly to the nucleus, so that the effective atomic orbital shrinks in space. This decreases the potential energy and increases the kinetic energy, roughly equally. If we model the orbital by a single exponential $\exp(-\zeta r)$, the effective charge ζ increases from 1 in the bare-atom case to $1{\cdot}193$ for the molecule. The decisive effect causing the necessary decrease in total energy is the decrease in kinetic energy in the overlap region. The energy arguments work exactly in reverse for the antisymmetric combination, which is unbound.

What do we expect to see in the spherically-averaged momentum density observed by EMS? First, very near the nuclei, corresponding to very large momenta, each electron experiences the attraction of one nuclear charge, as in the hydrogen atom. At very large distances, corresponding to almost-zero momentum, two electrons experience two relatively-close nuclear charges as in the helium atom. The momentum density at these extremes should be similar to that of the corresponding atom. The momentum density at intermediate momenta should be characteristic of the effective nuclear charge ζ. This is seen in Fig. 1, which compares momentum densities for the hydrogen molecule (Dey *et al.* 1975) with those of the hydrogen (Lohmann and Weigold 1981) and helium (McCarthy and Weigold 1976) atoms. The momentum densities are arbitrarily normalised to the same number at zero momentum to facilitate comparison.

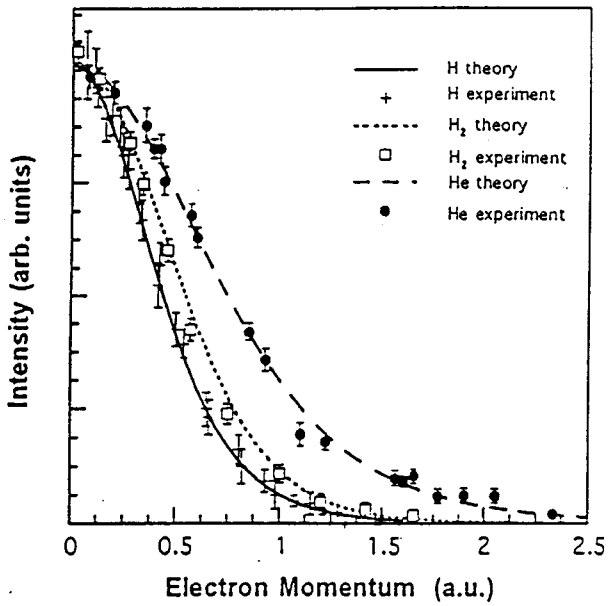

Fig. 1. Momentum-density profiles for the hydrogen and helium atoms and the hydrogen molecule.

3. One-dimensional Model of a Solid

At an early stage in the practical realisation of solid-state EMS in the Electronic Structure of Materials Centre, we asked ourselves what an electron orbital in a solid looks like and how it is related to a molecular orbital. Since EMS measures the density of absolute momentum q for a given one-electron energy eigenvalue ϵ, it makes sense to investigate the question in a one-dimensional model (Vos and McCarthy 1995). We chose an extension of the hydrogen molecule to a linear chain of hydrogen atoms, initially with spacing equal to that of the hydrogen molecule. We calculated molecular orbitals with the SCF program GAMESS (Schmidt *et al.* 1987), using a basis of s and p functions appropriate to the hydrogen molecule, centred at the nuclei. For an even number N of atoms there are $N/2$ doubly-occupied orbitals.

We first investigate the arbitrarily-normalised momentum density of each orbital for the direction of the chain, observing how its shape changes with increasing N and how the momentum densities for the $N/2$ orbitals are related. This is shown in Fig. 2 for N increasing from 2 to 32. For $N = 2$ the density is that of an oriented hydrogen molecule. If N is a multiple of 4 there are two types of density profile, one with an antinode and one with a node at the origin, corresponding to coordinate-space orbitals that are symmetric and antisymmetric about the chain centre. The density profile has $N/4$ lobes. The lobe for highest momentum is largest and begins to dominate as N increases. The model has not introduced orbital gradients qualitatively different from the hydrogen molecule, so there is no significant momentum density above $q = 1{\cdot}5$ a.u. Hence, as N increases, the large lobe for maximum q must decrease in width, approximating a delta function, so that the orbital approximates a momentum eigenfunction, that is the orbital of a free electron.

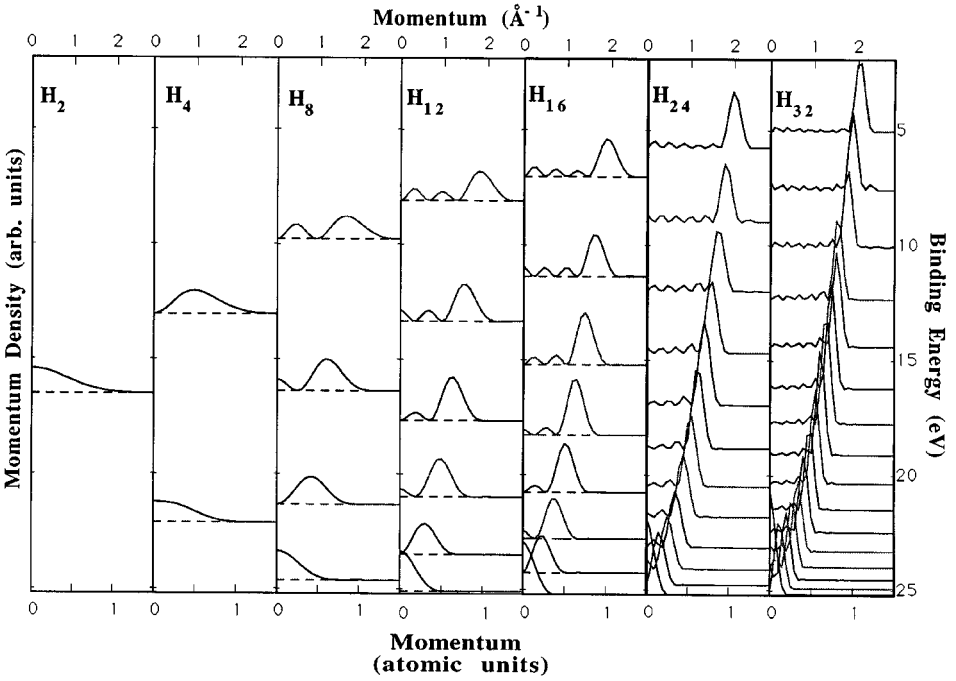

Fig. 2. Momentum density of the molecular orbitals for uniform linear hydrogen chains of the indicated lengths. The momentum profiles are offset vertically by an amount proportional to the energy.

In Fig. 2 the orbital densities are offset vertically by an amount proportional to the energy eigenvalue ϵ. This enables us to see that the energy–momentum density approaches the situation where the orbital densities coalesce to give a parabolic dispersion relation

$$\epsilon = \epsilon_0 + q^2/2m^*. \tag{2}$$

This is the dispersion relation of free electrons, except that the effective mass m^* is modified by the lattice to be slightly less than the free-electron value 1 in atomic units. Fig. 3 shows that the momentum-density profile for $N = 32$ has a sharp cutoff, reminiscent of the Fermi momentum of a free-electron metal, in contrast to the diffuse high-momentum region of atomic hydrogen.

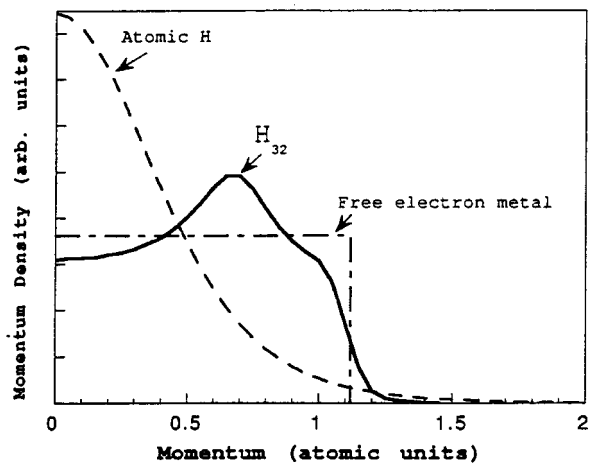

Fig. 3. Momentum density of the H_{32} molecule compared with that of atomic hydrogen and a free-electron metal.

Fig. 4 shows that what we have learnt from the orbital momentum profiles is confirmed when the orbitals for $N = 32$ are plotted in coordinate space. The overall structure of an orbital is a standing wave. All the occupied eigenstates of a free particle in a box of length equal to that of the chain, indexed from 1 to 16 in ascending energy order, are represented. Each standing wave has 32 ripples that are what remains of the effect of the 32 individual nuclei. In fact each atomic orbital overlaps several nuclei, so that the electron motion is governed mainly by the whole chain, rather than by an individual nucleus. In crystal language the highest-energy occupied orbital, the sixteenth, has 16 density lobes, each covering two unit cells.

A real-life example of the situation represented by the uniformly-spaced chain is a free-electron metal such as aluminium, whose experimental energy–momentum density is shown in Fig. 5 (Canney *et al.* 1997). The dispersion parabola is uniformly occupied up to the Fermi level. There are two effects of multiple scattering of the probe electrons. The parabola is repeated at energies about 15 eV and 30 eV lower, due to the observation of events in which one or two plasmons have been excited. These are eigenstates of the collective motion of the plasma set up by the essentially-free electrons in the positive-ion background. The energy–momentum density is broadened in momentum by elastic scattering from atomic cores, which recoil, setting up vibrations or phonons. These excitation energies are not resolved, so that the effect is incoherently elastic.

In the next example we double the size of the unit cell by alternating the spacing in the sequence a, b, a, b ... . Now each space-density lobe of the highest occupied orbital covers exactly one unit cell, the maximum negative charge density

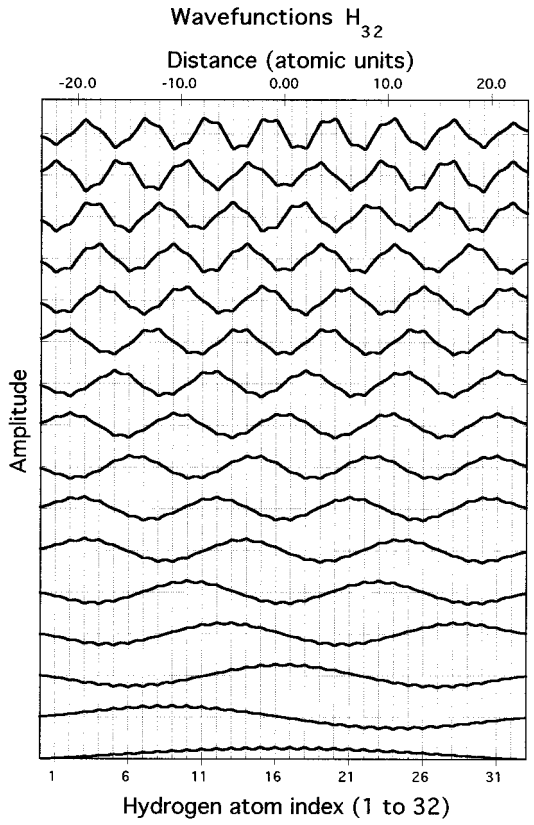

Fig. 4. Coordinate-space orbitals for H_{32} from 1 to 16 with increasing energy.

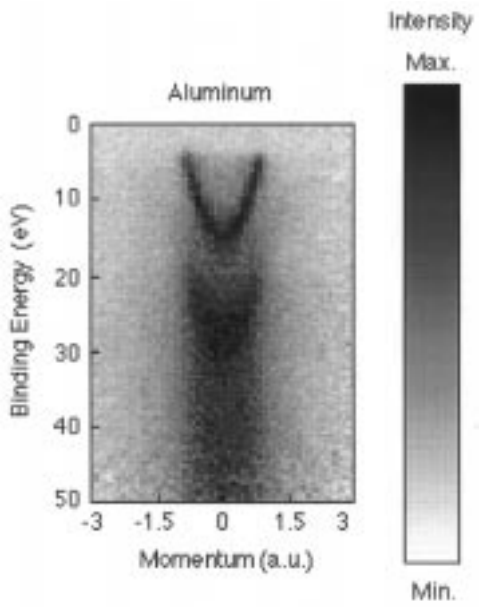

Fig. 5. Experimental energy–momentum density of valence and plasmon-excited states in polycrystalline aluminium.

being at the centre of positive charge of the unit cell. Consider the seventeenth orbital, which is unoccupied in the $N = 32$ case. The negative charge density now has a minimum at the charge centre of each unit cell near the centre of the chain. It is nearly minimum at the centre of neighbouring unit cells and would be minimum in an infinite chain. This phase-change situation is responsible for a large energy difference between the highest occupied orbital and the lowest unoccupied orbital, namely the band gap.

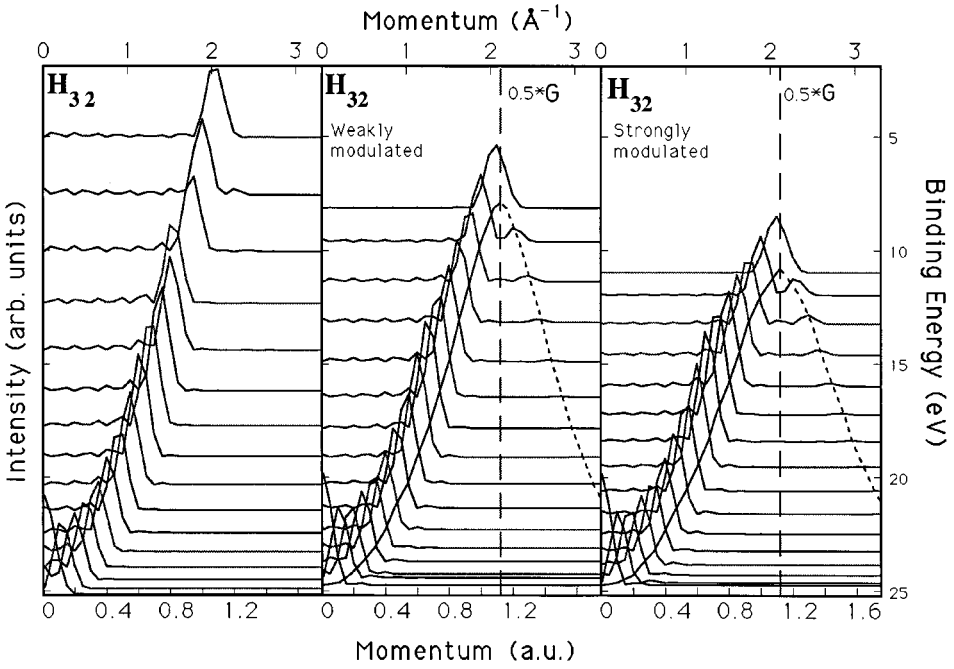

Fig. 6. Momentum density of the orbitals of H_{32} with modulation of the internuclear spacing as described in the text. Solid curves indicate the band shape inferred from the peak positions. The broken curves indicate the band plotted for negative momenta after adding a reciprocal-lattice vector.

The energy–momentum density plot of Fig. 6 shows that the band gap increases as a changes from $1{\cdot}4$ to $1{\cdot}2$ to 1 a.u. and b from $1{\cdot}4$ to $1{\cdot}6$ to $1{\cdot}8$ a.u., that is, as the modulation of the spacing increases from zero and the unit cells become more isolated from each other. The boundary of the first Brillouin zone is at half a reciprocal-lattice vector G from the centre of the zone where $q = 0$. The unit-cell length is $2{\cdot}8$ a.u., so that $0{\cdot}5G = 0{\cdot}5 \times 2\pi/2{\cdot}8$ a.u. $= 1{\cdot}1$ a.u. The solid curve in Fig. 6 connects the energy points for the main momentum-density lobes. It is the dispersion curve of the band in the first Brillouin zone. Note that there are secondary maxima in the second zone, for which the dispersion curve is the broken line. Their intensity increases with the spacing modulation. In the finite crystal, reflection at the boundary produces standing waves for q and $-q$. In an infinite crystal there are no boundaries and the orbital can be described either by q or $-q$. The secondary maxima can be interpreted as the $-q$ component shifted by a reciprocal-lattice vector due to interaction with the lattice.

A solid with orbitals fully occupied up to the band gap and unoccupied above it is a semiconductor. A real-life example is amorphous silicon, for which the energy–momentum density is averaged over unit-cell orientations. It is shown in Fig. 7, with the experiment in the first panel and a SCF simulation of the experiment in the second panel (Vos *et al.* 1995). Experimental and theoretical dispersion relations are shown in the third panel. The similarity to the model calculation of Fig. 6 is striking.

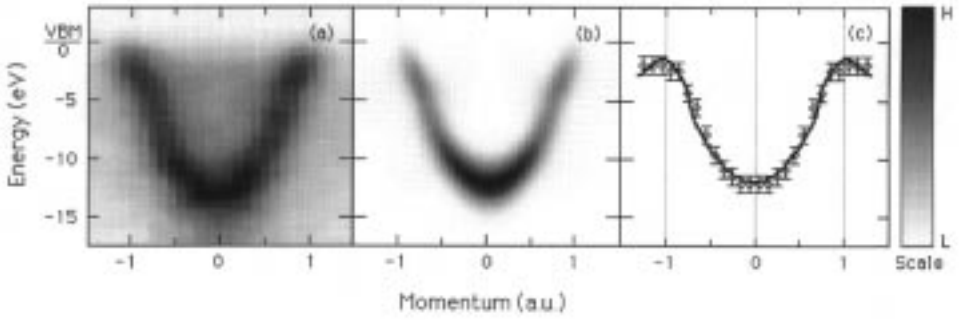

Fig. 7. (*a*) Energy–momentum density of the valence band of amorphous silicon; (*b*) the SCF calculation for polycrystalline silicon with appropriate broadening; and (*c*) comparison of the observed and calculated dispersion.

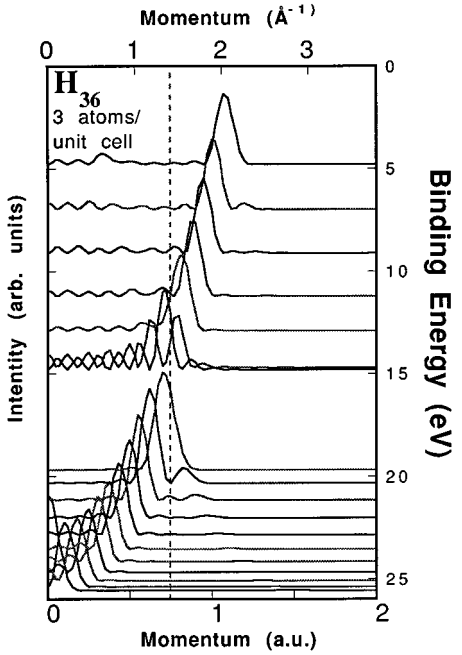

Fig. 8. Momentum density of the orbitals for H_{36} with three atoms per unit cell.

We can learn more by considering a modulation of the chain that gives three atoms per unit cell. The internuclear pattern is a, a, b, a, a, b ... , with $a = 1{\cdot}6$ a.u. and $b = 1{\cdot}0$ a.u. We now choose $N = 36$ to accommodate an even number 12 of unit cells. Now we expect a filled band in the first Brillouin zone where

the number of orbitals is equal to the number of unit cells. The remaining orbitals will be occupied above the band gap, forming a second band in the second zone. The calculated energy–momentum density is shown in Fig. 8. In fact the band gap starts at orbital 11 and the second band at 14. There are two orbitals of almost-equal energy in the band gap. The coordinate-space picture of Fig. 9 shows that the density of orbitals 12 and 13 peaks near the ends of the chain. They correspond to surface states in the band gap, a well-known solid-state phenomenon.

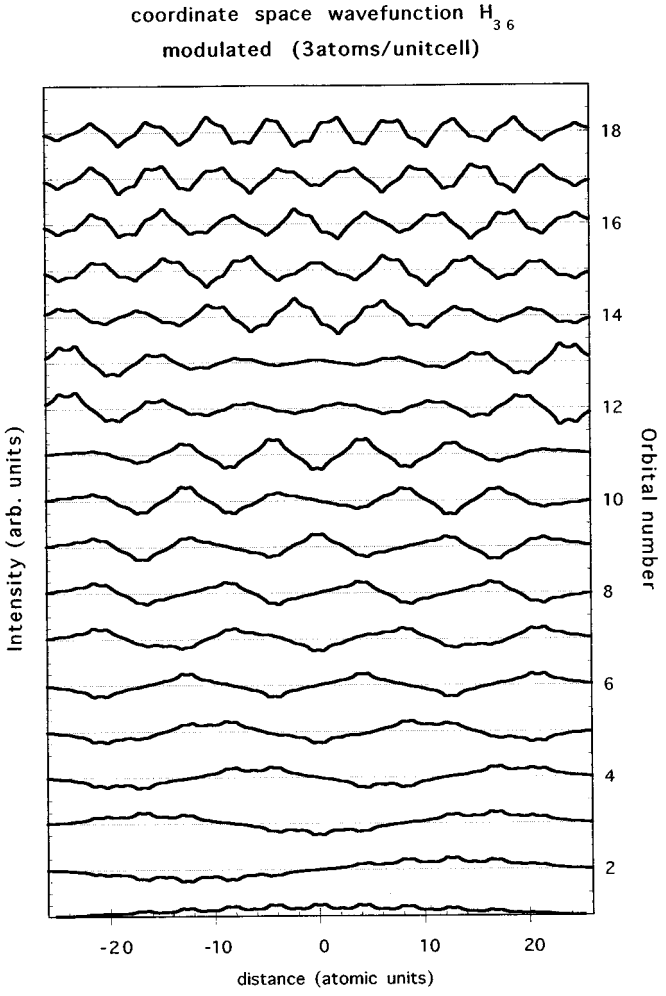

Fig. 9. Coordinate-space orbitals corresponding to Fig. 8.

A solid with a larger unit cell that exhibits analogous band behaviour is silicon carbide. Its experimental and theoretical energy–momentum diagrams and dispersion relations (Canney *et al.* 1997) are shown in Fig. 10, again confirming the prediction of the one-dimensional model. Secondary maxima are again observed, both in the model and the silicon-carbide example.

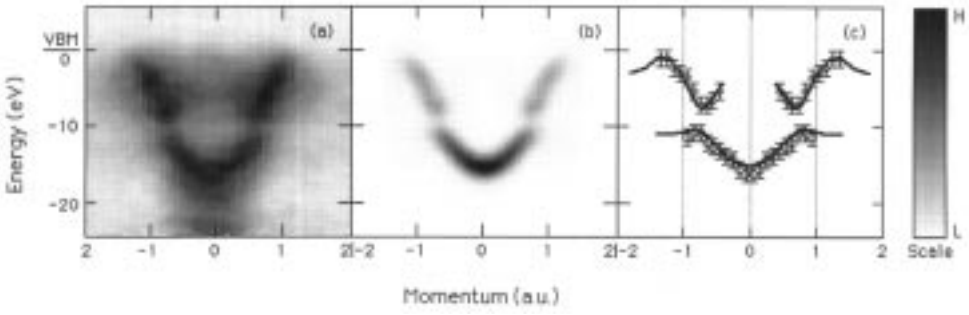

Fig. 10. Experimental and SCF energy–momentum densities for silicon carbide, corresponding to Fig. 7.

4. Crystal Orbitals in Three Dimensions

The experimental examples in the previous section and their SCF calculations are further understood by considering the form of a coordinate-space orbital of a large three-dimensional crystal, and transforming it to momentum space. A crystal comprises N identical unit cells whose centres define the lattice vectors $\mathbf{R}_n$. The symmetry index α describes the symmetry of an orbital with respect to the unit cell. The orbital with symmetry α for crystal momentum $\mathbf{k}$ is

$$\Psi_{\alpha\mathbf{k}}(\mathbf{r}) = N^{-1/2} \sum_{n=0}^{N-1} \psi_\alpha(\mathbf{r} - \mathbf{R}_n) \exp(i\mathbf{k} \cdot \mathbf{R}_n). \tag{3}$$

This is a Bloch function, which has the translational symmetry of the crystal lattice. It is described by equation (8·6) of Ashcroft and Mermin (1976). It is the obvious extension of the orbitals of, for example, Fig. 4. The standing wave, modulated by a function related to the unit cell, is replaced by a plane wave with the crystal momentum $\mathbf{k}$, modulated by the unit-cell orbital $\psi_\alpha(\mathbf{r})$. The unit-cell orbital is similar to a molecular orbital, considering the unit cell as a molecule that is repeated to form the crystal. Its boundary conditions, however, describe the smooth joining of orbitals for adjacent unit cells, rather than the decay of the orbital outside the molecule. The crystal momentum $\mathbf{k}$ is a set of three continuous quantum numbers, analogous to the index of the standing wave. The addition of a reciprocal-lattice vector to $\mathbf{k}$ makes no difference to the orbital.

The momentum-space orbital is the Dirac–Fourier transform of $\Psi_{\alpha\mathbf{k}}(\mathbf{r})$:

$$\begin{aligned} \Phi_{\alpha\mathbf{k}}(\mathbf{q}) &= N^{-1/2}(2\pi)^{-3/2} \int d^3r \exp(-i\mathbf{q} \cdot \mathbf{r}) \sum_{n=0}^{N-1} \psi_\alpha(\mathbf{r} - \mathbf{R}_n) \exp(i\mathbf{k} \cdot \mathbf{R}_n) \\ &= N^{\frac{1}{2}} \phi_\alpha(\mathbf{q}) \delta_{\mathbf{k}-\mathbf{q}}. \end{aligned} \tag{4}$$

Here $\phi_\alpha(\mathbf{q})$ is the momentum-space orbital of the unit cell,

$$\phi_\alpha(\mathbf{q}) = (2\pi)^{-3/2} \int d^3r \exp(-i\mathbf{q} \cdot \mathbf{r}) \psi_\alpha(\mathbf{r}). \tag{5}$$

Its absolute square gives the density for the momentum $\mathbf{q}$, corresponding to the energy $\epsilon(\mathbf{q})$ given by the dispersion relation. The factor

$$\delta_{\mathbf{k}-\mathbf{q}} = N^{-1} \sum_{n=0}^{N-1} \exp\bigl[i(\mathbf{k}-\mathbf{q})\cdot\mathbf{R}_n\bigr], \tag{6}$$

for a large crystal, equates the crystal momentum $\mathbf{k}$ to the observed momentum $\mathbf{q}$.

5. Real Example of a Transitional Stage

We have considered a large molecule consisting of a chain of unit cells as an example of the transition from a molecule to a solid. In all our examples the internuclear bonds have been identical sigma bonds. The corresponding bands are sigma bands.

An interesting example is graphite, where valence s and p electrons form sigma bonds resulting in hexagonal unit cells on a plane sheet. On each nucleus there are additional p electrons whose orbital lobes are normal to the plane. They form pi bonds that loosely bind graphite sheets. The p orbitals and pi bands are characterised by zero density at zero momentum. The experimental sigma (lower) and pi (upper) bands of polycrystalline graphite (Vos *et al.* 1994) are shown in Fig. 11*a*, where their energy–momentum densities are averaged over orientations.

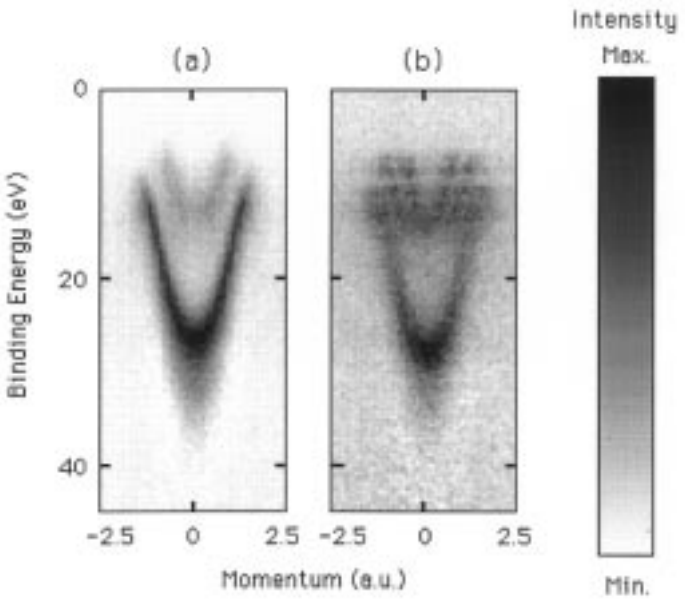

Fig. 11. Experimental energy–momentum density for (*a*) amorphous graphite and (*b*) fullerene.

A molecule that can be considered as a finite number of graphite cells spread evenly over all orientations is fullerene. It is formed by taking 60 carbon atoms in a finite graphite sheet and warping it into a symmetric, almost spherical

shell to form a molecule. The warping process reduces some faces to five vertices, but this does not invalidate the picture. Fig. 11*b* shows the experimental energy–momentum density of fullerene (Vos *et al.* 1997). It is very similar to that of graphite except that the pi band is split into two because p lobes inside and outside the shell are different. In the finite models of Figs 2, 6 and 8 the inter-orbital energy spacing is largest for the highest energy and decreases as the energy decreases. For fullerene the inter-orbital energy spacing is large enough to be resolved in the experiment for the uppermost orbitals. Each orbital has density maxima on the band dispersion curves. Lower orbital energies are not resolved and their observed densities coalesce to give a picture identical to graphite.

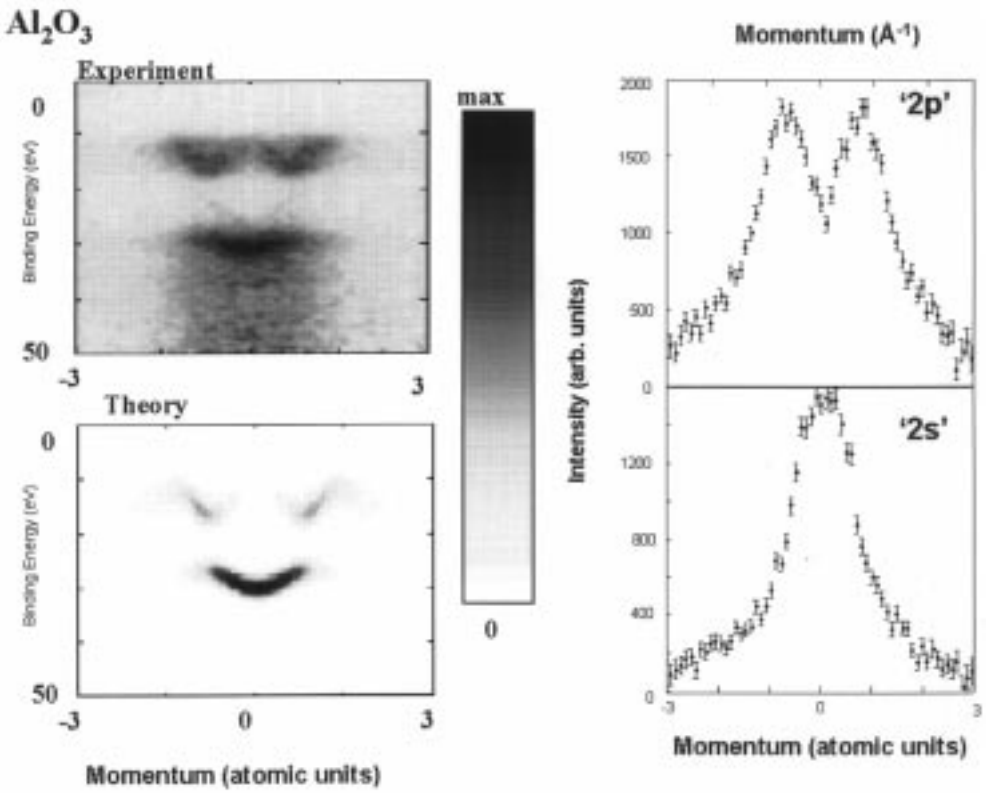

Fig. 12. Experimental and SCF energy–momentum densities for the valence bands of alumina (*left*) and the corresponding energy-integrated momentum densities (*right*).

6. An Ionic Solid

Alumina is an ionic insulator with the chemical composition Al_2O_3. The six $n = 3$ valence electrons of two aluminium atoms fill the two valence holes of each of three oxygen atoms, producing the $n = 2$ electronic configuration of neon for each ion. The negative oxygen ion is larger and its valence electrons are responsible for the electronic structure observed by EMS (Guo *et al.* 1996). The experimental and SCF energy–momentum densities are shown in Fig. 12. Two bands are observed, corresponding to the s (lower) and p (upper) orbitals of an inert-gas atom. Also shown in Fig. 12 are the momentum densities, summed over energy for each band, from which we derive effective rms radii $1{\cdot}2$ a.u. for '2s' and $1{\cdot}4$ a.u. for '2p'. The rms radii of the ions are considerably less than the average spacing $a = 4{\cdot}7$ a.u. of the oxygen ions. We may consider an alumina target as a collection of randomly-oriented linear molecules with this spacing.

Instead of the atomic s orbitals considered in our linear hydrogen chain we have ionic s and p orbitals. The other major difference is that in the hydrogen chain there was considerable overlap between the atomic orbitals on different centres, while there is very little overlap for alumina. For this reason the electrons do not readily migrate through the solid, although the existence of solid-state effects is shown by the fact that the bands are not entirely flat, as for isolated ions, but have maximum and minimum energies. There is one minimum for the s band, which corresponds to the parabolic sigma band of a 'metal' with a very large effective mass. The p band has two minima, equally spaced on either side of the zero-momentum node.

The structure can be explained on the basis of a linear chain. For s orbitals the lowest energy occurs for the combination where they add in phase, since the interference between the nuclei is then constructive. The Dirac–Fourier transform averages the orbital over all space. Since there is a large constant component the momentum density of the in-phase bonding orbital will peak at zero momentum. The least-bound orbital is the antisymmetric combination. Its wavelength is $2a$ and its Dirac–Fourier transform peaks at $q = 2\pi/2a = 0{\cdot}67$ a.u., which is close to the experimental value. Combinations of atomic orbitals that are between the symmetric and antisymmetric extremes correspond to intermediate momentum and energy values.

Since an atomic p orbital has opposite signs on opposite sides of the centre, the strongest bonding combination is the antisymmetric one so that energy minima are expected at $0{\cdot}67$ a.u., in agreement with experiment. The symmetric sum has wavelength a and hence its momentum density peaks at $q = 2\pi/a = 1{\cdot}34$ a.u., again in agreement with experiment.

7. Conclusion

We have shown how the electronic structure of different types of solid can be understood in terms of molecular orbitals. Because EMS directly observes the momentum density of orbitals, the experimental quantity most closely related to their electronic structure, it is able to confirm detailed qualitative predictions based on an understanding of their structure and relationship.

Acknowledgments

The Electronic Structure of Materials Centre was a Special Research Centre supported by the Australian Research Council from 1988 to 1996. We acknowledge the contribution of the entire staff of the Centre to the work described here.

References

Ashcroft, N. W., and Mermin, N. D. (1976). 'Solid State Physics' (Holt, Rinehart and Winston: New York).

Cai, Y. Q., Vos, M., Storer, P. J., Kheifets, A. S., McCarthy, I. E., and Weigold, E. (1995). *Phys. Rev.* **51**, 3449.

Canney, S. A., Vos, M., Kheifets, A. S., Clisby, N., McCarthy, I. E., and Weigold, E. (1997). *J. Phys. Condens. Matter* **39**, 1931.

Dey, S., McCarthy, I. E., Teubner, P. J. O., and Weigold, E. (1975). *Phys. Rev. Lett.* **34**, 782.

Guo, X., Cannery, S. A., Kheifets, A. S., Vos, M., Fang, Z., Utteridge, S., McCarthy, I. E., and Weigold, E. (1996). *Phys. Rev.* B **54**, 17943.

Lohmann, B., and Weigold, E. (1981). *Phys. Lett.* A **66**, 139.

McCarthy, I. E., and Weigold, E. (1976). *Phys. Rep.* C **27**, 275.

McCarthy, I. E., and Weigold, E. (1991). *Rep. Prog. Phys.* **54**, 789.

Ruedenberg, K. (1962). *Rev. Mod. Phys.* **34**, 326.

Schmidt, M. W., Boatz, J. A., Baldridge, K. K., Koseki, S., Gordon, M. S., Elbert, T., and Lam, B. (1987). *QCPE Bulletin* **7**, 115.

Vos, M., and McCarthy, I. E. (1995). *Rev. Mod. Phys.* **67**, 713.
Vos, M., Canney, S. A., McCarthy, I. E., Utteridge, S., Michalewicz, M. T., and Weigold, E. (1997). *Phys. Rev.* B **56**, 1309.
Vos, M., Storer, P. J., Cai, Y. Q., Kheifets, A. S., McCarthy, I. E., and Weigold, E. (1995). *J. Phys. Condens. Matter* **7**, 279.
Vos, M., Storer, P. J., Canney, S. A., Kheifets, A. S., McCarthy, I. E., and Weigold, E. (1994). *Phys. Rev.* B **50**, 5635.

Manuscript received 1 October 1998, accepted 1 February 1999